Comparison of gated and dynamic cone-beam CT reconstruction methods

1 Introduction

In the past few years, there has been an increasing interest of the radiation oncology community in cone-beam computed tomography (CT) scanners integrated into the gantry of medical linear accelerators. This imaging device allows to acquire CT images of the patient in treatment position. Unfortunately, like for other CT scanners, the respiratory motion of the patient during acquisition causes artifacts such as blur, streaks and bands. The current methods available to correct these artifacts can be categorized in 3 classes, depending if they use (1) no motion information, (2) only simplified motion information like a respiratory signal, in which case the method is called respiratory-correlated or gated imaging [2, 5, 7, 10], or (3) precise motion information like a dense vector field or a B-spline model, in which case the method is called dynamic reconstruction [1, 4, 6].

The respiratory-correlated or gated technique consists in selecting a subset of the cone-beam projections, on the basis of their position in the respiratory cycle, and to use these projections in a conventional static reconstruction algorithm to obtain an image of a respiratory instant. On the contrary, dynamic reconstruction uses all the projections, but the reconstruction algorithm is modified to compensate for the motion of the thorax. Both methods have been studied in the past but, to our knowledge, they have not been directly compared.

In this study, we compared the gated and dynamic CT reconstructions of a moving mechanical phantom from cone-beam projections acquired using a linear accelerator with a kV cone-beam scanner. The motion was sinusoidal in the cranio-caudal direction only. This made it easy to extract both the respiratory signal and the 4D motion, which would not have been the case for real patient acquisitions. The resulting CT images were compared quantitatively, by reference to the static CT reconstruction from the set of cone-beam projections obtained with the fixed platform.

2 Material and methods

2.1 Mechanical phantom description

A phantom was placed on a mobile platform. The platform translated in the cranio-caudal direction with a sinusoidal motion. The peak-to-peak amplitude was 14 mm and the period was 3.5 seconds. The phantom was composed of a stack of three $20 \times 20 \times 2$ cm^3 slabs of wood ($\mu \simeq 0.4$ g.cm^{-3}) with a $4 \times 4 \times 2$ cm^3 cube of polyethylene ($\mu = 0.98$ g.cm^{-3}) inserted in the center of the middle slab (figure 1).

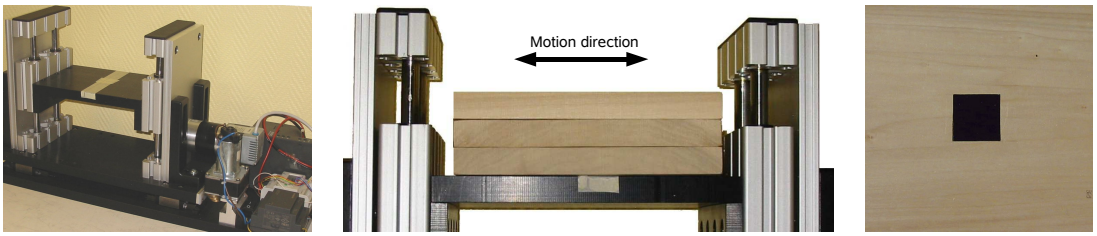

(a) (b) (c)

Figure 1: Experimental set up composed of (a) a mobile platform, on top of which is (b) a phantom composed of three wooden slabs with (c) a polyethylene cube inserted in the center of the middle slab.

2.2 Cone-beam acquisitions

The cone-beam CT images were acquired with the Elekta Synergy system™(Elekta Oncology Systems Ltd., Crawley, West Sussex, United Kingdom). We acquired around 650 projections along a full circular trajectory with the kV beam centered on the isocenter and the maximum gantry rotation speed, i.e. 2 minutes per acquisition. Projections were 40.9×40.9 cm^2 in size, with a resolution of 512×512 pixels. Three acquisitions of the phantom were performed: two with the platform being fixed at its extreme positions and one with the platform moving.

2.3 Motion extraction

Respiratory signal We manually selected the projections corresponding to the extreme positions of the phantom in its periodic cycle by going through the sequence of projections. The associated relative acquisition times were retrieved from the cone-beam database and a sinusoid was automatically fitted to these positions to obtain the respiratory signal (figure 2).

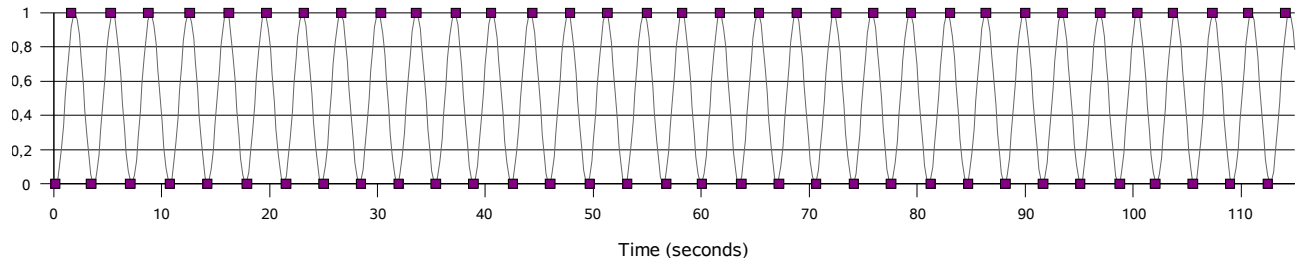

Figure 2: The manually selected points (squares) with the fitted sinusoid (line). This sinusoid represents the respiratory signal in this study.

4D motion The motion of the phantom was a simple translation. We manually extracted the positions of the corners of the polyethylene cube from the two CT images of the static phantom in its two extreme positions. The global translation vector was obtained by computing the average of the vectors resulting from the subtraction between couples of landmarks.

A 4D motion $\Phi : \mathbb{R}^3 \times \mathbb{R} \mapsto \mathbb{R}^3 \mid y = \Phi(x,t) = \Phi_t(x)$ maps the physical correspondence of each 3D point $y = \Phi_t(x)$, at any time t, and of a 3D point x at a reference time t_0. Φ_t is obtained by weighting the global translation vector by the respiratory signal value at time t.

2.4 Reconstruction methods

Static reconstruction The reconstruction used in this study was the analytical algorithm proposed by Feldkamp et al [3]. The artifact due to the truncation of the cone-beam projections was partially corrected using the heuristic method described by Ohnesorge et al [8].

Gated reconstruction The gating window determines which projections are used in the reconstruction process according to the respiratory signal. We used a gating window centered on the extreme position corresponding to the reference volume t_0, with a fixed width of 20% of the peak-to-peak amplitude of the respiratory signal. A previous study has demonstrated the limited impact of the gating window width on the quality of the reconstructed image, particularly when the motion is regular.

Dynamic reconstruction Dynamic reconstruction consists in integrating the 4D motion in the reconstruction process. We used the heuristic adaptation of the Feldkamp algorithm proposed in several past studies [4, 6, 9]. This adaptation consists in warping the backprojection of each filtered projection using the transformation Φ_t^{-1}, where t is the time of the acquisition of the cone-beam projection. The warp is implemented using Φ_t with an inverse mapping, which guarantees that all voxels of the warped backprojection are computed. The reconstructed volume is then the volume at time t_0.

2.5 Criteria

For quantitative analysis of the reconstructions, three criteria previously defined in the literature were applied to a region of interest including only the polyethylene cube and wood.

- The blur criterion (BC) proposed by Kriminski et al [5]. This method aims to quantify the blur independently from the noise by using an appropriate energy function for a binary segmentation robust to noise. The optimal energy is used as a criterion.

- The signal-to-noise ratio: $\mathrm{SNR(dB)} = 20 \log_{10} \frac{A_{\mathrm{signal}}}{A_{\mathrm{noise}}}$ where $A_I = \sqrt{\frac{1}{P} \sum_{i=1}^{P} x_i^2}$ is the root mean square of the intensity of the P pixels in image I; the *signal* is the reference, i.e. the CT image recontructed when the platform is fixed, and the *noise* is the difference between the reconstruction to be evaluated and the *signal*.

- The contrast-to-noise ratio: CNR $=\mid \mu_{\text{fg}} - \mu_{\text{bg}} \mid / \sigma_{\text{bg}}$ where μ_R and σ_R are the mean and the standard deviation of the voxel values in region R, and fg and bg are the foreground and the background resulting from the segmentation performed during the measurement of the blur criterion.

3 Results and discussion

The CT images obtained with the different reconstruction algorithms and the mobile platform can be visually compared with the CT image obtained with the static reconstruction and the fixed platform (figure 3). This comparison can be linked with the quantitative results obtained using the three criteria (figure 4).

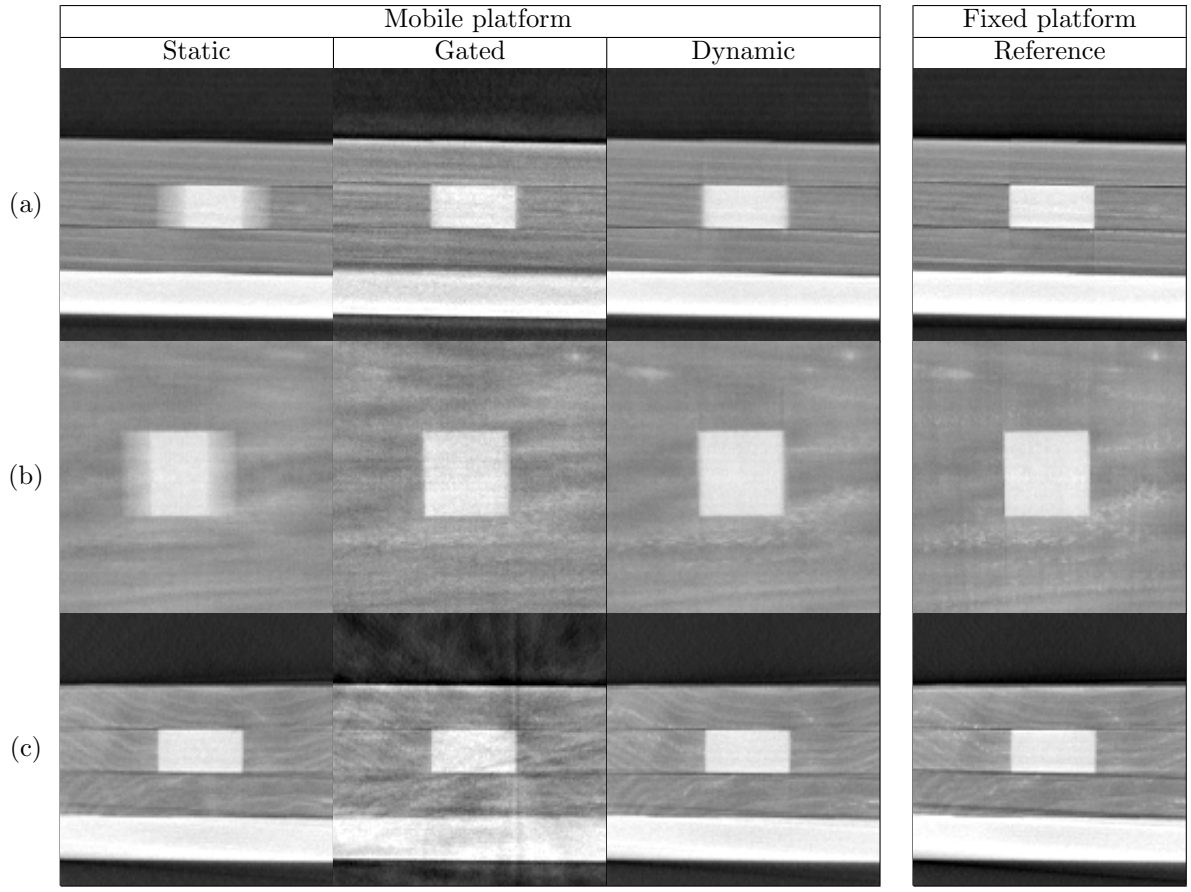

Figure 3: (a) Sagittal, (b) coronal and (c) transverse slices of the CT images built with static reconstruction, gated reconstruction or dynamic reconstruction from the set of cone-beam projections of the mobile platform. The reference is the CT image obtained when the platform is fixed.

For radiotherapy purposes, the first artifact to be corrected is the blur because it is the most disturbing factor interfering with the crucial contouring step. The task consists in segmenting the region of interest. We used Kriminski's blur criterion to evaluate it independently from other artifacts. Both gated and dynamic reconstructions corrected the strong blur artifact of static reconstruction (figure 3). The delineation of the polyethylene cube was easier and we obtained a blur criterion value very close to the reference value in both cases (figure 4).

For gated reconstruction, the selection of only a small subset of the cone-beam projections lead to other types of artifacts such as streaks and bands (figure 3). Such noise can be disturbing in radiotherapy, for example for the contouring of non-contrasted regions of interest or dose calculation. Adaptations of the acquisition protocol have been proposed such as the correction of these artifacts by the acquisition of more projections, either through slowing the gantry [10] or performing more than one rotation [7]. But these adaptations induce the delivery of a higher dose to the patient.

Artifacts were corrected by dynamic reconstruction because the method used all the cone-beam projections. The result was visually very close to the reference (figure 3). Quantitatively, the signal-to-noise ratio and the contrast-to-noise ratio confirmed that dynamic reconstruction provides images closer to the reference than gated reconstruction (figure 4).

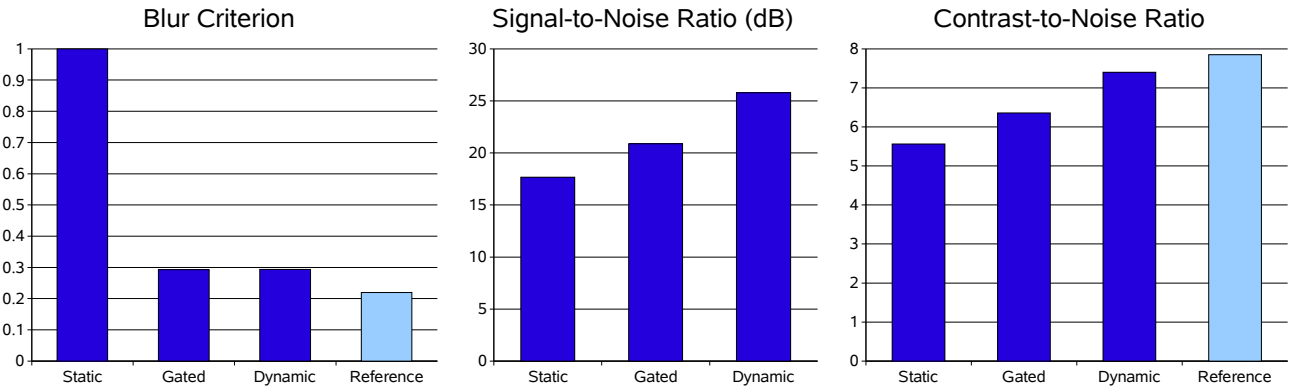

Figure 4: Quantitative evaluation of the static, gated and dynamic reconstruction algorithms from the set of cone-beam projections obtained with the mobile platform using our three criteria (dark blue). The static reconstruction with the fixed platform (light blue) is used as reference. The signal-to-noise ratio is computed using the reference reconstruction as a reference signal.

4 Conclusion

We have studied two different algorithms for the management of motion in CT reconstruction from cone-beam projections acquired with a slowly rotating scanner. Acquisitions have been performed on a dynamic mechanical phantom and evaluated qualitatively and quantitatively. Gated reconstruction corrects blur artifacts but yields noisy results. Dynamic reconstruction gives results close to the CT image obtained when the platform is fixed.

However, the use of dynamic reconstruction on patient data is much more complicated because it requires using the 4D motion model during the acquisition step. But promising solutions have been proposed in the past to obtain such 4D motion models. Our future studies will adress the reconstruction of simulated and real patient images with both analytic and algebraic methods.

References

[1] S. Bonnet, A. Koenig, S. Roux, P. Hugonnard, R. Guillemaud, and P. Grangeat. Dynamic X-ray computed tomography. *Proceedings of the IEEE*, 91(10):1574–1587, 2003.

[2] L. Dietrich, S. Jetter, T. Tücking, S. Nill, and U. Oelfke. Linac-integrated 4D cone beam CT: first experimental results. *Physics in Medicine and Biology*, 51(11):2939–2952, 2006.

[3] L.A. Feldkamp, L.C. Davis, and J.W. Kress. Practical cone-beam algorithm. *Journal of Optical Society of America A*, 1(6):612–619, 1984.

[4] P. Grangeat, A. Koenig, T. Rodet, and S. Bonnet. Theoretical framework for a dynamic cone-beam reconstruction algorithm based on a dynamic particle model. *Physics in Medicine and Biology*, 47(15):2611–2625, 2002.

[5] S. Kriminski, M. Mitschke, S. Sorensen, N.M. Wink, P.E. Chow, S. Tenn, and T.D. Solberg. Respiratory correlated cone-beam computed tomography on an isocentric C-arm. *Physics in Medicine and Biology*, 50(22):5263–5280, 2005.

[6] T. Li, E. Schreibmann, Y. Yang, and L. Xing. Motion correction for improved target localization with on-board cone-beam computed tomography. *Physics in Medicine and Biology*, 51(10):253–267, 2006.

[7] T. Li, L. Xing, P. Munro, C. McGuinness, M. Chao, Y. Yang, B. Loo, and A. Koong. Four-dimensional cone-beam computed tomography using an on-board imager. *Medical Physics*, 33(10):3825–3833, 2006.

[8] B. Ohnesorge, T. Flohr, K. Schwarz, J.P. Heiken, and K.T. Bae. Efficient correction for CT image artifacts caused by objects extending outside the scan field of view. *Medical Physics*, 27(1):39–46, 2000.

[9] C.J. Ritchie, C.R. Crawford, J.D. Godwin, K.F. King, and Y. Kim. Correction of computed tomography motion artifacts using pixel-specific back-projection. *IEEE Transactions on Medical Imaging*, 15(3):333–342, 1996.

[10] J.-J. Sonke, L. Zijp, P. Remeijer, and M. Van Herk. Respiratory correlated cone beam CT. *Medical Physics*, 32(4):1176–1186, 2005.